Inorganic Chemistry
Article

Inorg. Chem. **2010**, *49*, 2447–2456 **2447**
DOI: 10.1021/ic902317h

Tetra-2,3-pyrazinoporphyrazines with Externally Appended Pyridine Rings. 8. Central (Zn^{II}, Cu^{II}, $Mg^{II}(H_2O)$, Cd^{II}) and Exocyclic (Pd^{II}) Metal Ion Binding in Heteropentametallic Complexes from Tetrakis-2,3-[5,6-di(2-pyridyl)pyrazino]porphyrazine

Maria Pia Donzello,[†] Elisa Viola,[†] Xiaohui Cai,[‡] Luisa Mannina,*[,§] Claudio Ercolani,*[,†] and Karl M. Kadish*[,‡]

[†]*Dipartimento di Chimica, Università degli Studi di Roma "La Sapienza", P.le A. Moro 5, I-00185 Roma, Italy,* [‡]*Department of Chemistry, University of Houston, Houston, Texas, 77204-5003, and* [§]*Dipartimento di Chimica e Tecnologie del Farmaco, Università degli Studi di Roma "La Sapienza", P.le A. Moro 5, I-00185 Roma, Italy, and Istituto di Metodologie Chimiche, CNR, I-00016, Monterotondo Staz., Roma, Italy*

Received November 23, 2009

A series of heteropentametallic porphyrazine macrocycles, represented as $[(PdCl_2)_4LM]$, where L = dianion of tetrakis-2,3-[5,6-di(2-pyridyl)pyrazino]porphyrazine and M = Zn^{II}, Cu^{II} $Mg^{II}(H_2O)$ or Cd^{II}, were prepared by reaction of the corresponding mononuclear [LM] species, and their behavior was examined by UV−visible and NMR spectroscopy, electrochemistry, and thin layer spectroelectrochemistry in nonaqueous media. The $PdCl_2$ units in $[(PdCl_2)_4LM]$ are coordinated at the pyridine N atoms of the external dipyridinopyrazine fragments ("py-py" coordination) and are displaced out of the plane of the central pyrazinoporphyrazine macrocycle as verified by ^1H and ^{13}C NMR data on $[(PdCl_2)_4LZn]$. The same arrangement is also strongly suggested by similar NMR data on the Mg^{II} and Cd^{II} analogues. The predominant component in the synthesized materials among the four predictable macrocyclic isomers has the four exocyclic $N_{2(py)}PdCl_2$ square planar coordination sites on the same side of the central macrocyclic framework (4:0 isomer, C_{4v} symmetry), and this is accompanied by a minor isomeric component (2:2 cis or trans), in line with previous findings on the pentapalladated species $[(PdCl_2)_4LPd]$. IR, UV−visible, and NMR spectral data also provide evidence for transmetalation reactions of the type $[(PdCl_2)_4LMg(H_2O)] \rightarrow [(PdCl_2)_4LPd]$ and $[(PdCl_2)_4LCd] \rightarrow [(PdCl_2)_4LPd]$, with the amount of $[(PdCl_2)_4LPd]$ formed varying from batch to batch. Dissociation of the four exocyclic $PdCl_2$ units from $[(PdCl_2)_4LM]$ occurs in pyridine, but the compounds are stable in *N*,*N*-dimethylformamide (DMF) or dimethylsulfoxide (DMSO) and can be stepwise reduced via two one-electron reversible or quasi-reversible processes, prior to an irreversible electroreduction of the bound $PdCl_2$ group at more negative potentials. This metal-centered reduction leads to a $[LM]^{2-}$ product which is then further reduced to $[LM]^{3-}$ and $[LM]^{4-}$ at the electrode surface. The first two reductions of the heteropentametallic compounds are easier than those of the monometallic [LM] species but generally more difficult than reduction of the related octacationic $[L'M]^{8+}$ derivatives (L′ = the octamethylated free-base dianion) whose redox properties were previously reported. The Cd^{II} octacation $[L'Cd]^{8+}$, isolated as an iodide salt, was also synthesized for the first time in the current study, and its spectroscopic and electrochemical properties are compared to that of the previously examined analogues.

Introduction

In previous studies, we characterized the free-base macrocycle tetrakis-2,3-[5,6-di(2-pyridyl)pyrazino]porphyrazine,[1] $[LH_2]$, and a series of its metal derivatives. The investigated metallomacrocycles are represented as [LM] and $[L'M]^{8+}$ where M = $Mg^{II}(H_2O)$, Mn^{II}, Co^{II}, Cu^{II}, or Zn^{II} and L and L′ are the dianions of LH_2 and of its corresponding octamethylated species, respectively (see Scheme 1).[2,3] Coordination of one water molecule to Mg^{II} in the $[LMg(H_2O)]$ complex was previously reported.[2a] These metalloporphyrazines are easily prepared in moderate-to-high yield and generally have a prolonged stability in air (months/years) as well as a high thermal stability ($T > 300$ °C). Detailed

*To whom correspondence should be addressed. E-mail: claudio.ercolani@uniroma1.it (C.E.), kkadish@uh.edu (K.M.K.).

(1) Donzello, M. P.; Ou, Z.; Monacelli, F.; Ricciardi, G.; Rizzoli, C.; Ercolani, C.; Kadish, K. M. *Inorg. Chem.* **2004**, *43*, 8626.

(2) (a) Donzello, M. P.; Ou, Z.; Dini, D.; Meneghetti, M.; Ercolani, C.; Kadish, K. M. *Inorg. Chem.* **2004**, *43*, 8637. (b) Villano, M.; Amendola, V.; Sandonà, G.; Donzello, M. P.; Ercolani, C.; Meneghetti, M. *J. Phys. Chem. B* **2006**, *110*, 24534. (c) Viola, E.; Donzello, M. P.; Ciattini, S.; Portalone, G.; Ercolani, C. *Eur. J. Inorg. Chem.* **2009**, 1600.

(3) (a) Bergami, C.; Donzello, M. P.; Ercolani, C.; Monacelli, F.; Kadish, K. M.; Rizzoli, C. *Inorg. Chem.* **2005**, *44*, 9852. (b) Bergami, C.; Donzello, M. P.; Monacelli, F.; Ercolani, C.; Kadish, K. M. *Inorg. Chem.* **2005**, *44*, 9862.

Published on Web 01/26/2010

Scheme 1. Schematic Representation of the Neutral Complexes [LM][2a] and Their Corresponding Octacations [L′M]$^{8+}$ (Salted by I$^-$ Ions)[3b]

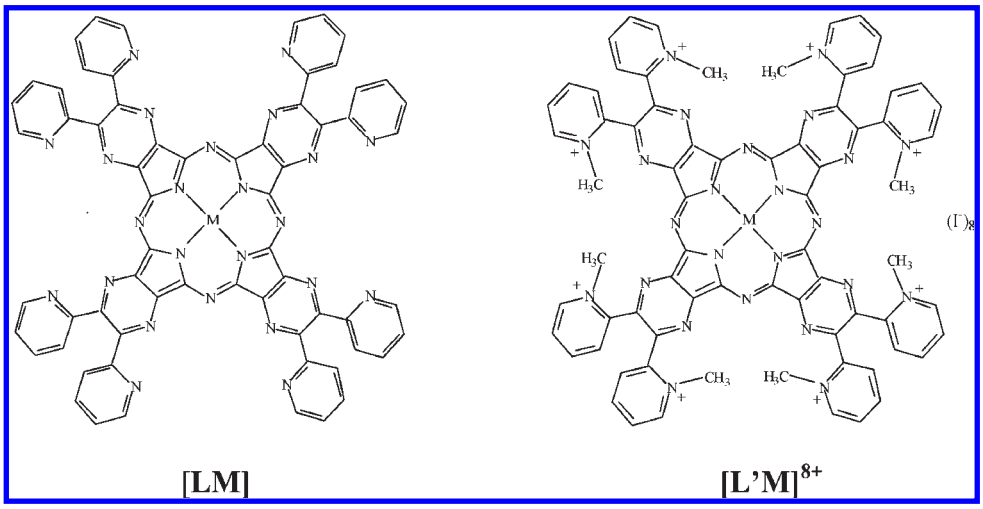

cyclic voltammetric and spectroelectrochemical studies indicated that the series of neutral [LM] complexes[2,3b] and their related octacations[3b] [L′M]$^{8+}$ both undergo stepwise one-electron reductions with formation of −1, −2, −3, and −4 charged species at potentials significantly shifted in a positive direction with respect to $E_{1/2}$ values for reduction of a related series of phthalocyanines.[4] This increased ease of reduction is due to their remarkable electron-deficient properties induced by the presence of the strongly electron-withdrawing, externally annulated "dipyridinopyrazine" fragments.

We also recently reported the synthesis and physicochemical behavior of the Pd^{II} complex [LPd], its related octacation, [L′Pd]$^{8+}$, and the neutral pentanuclear complex [$(PdCl_2)_4$-LPd] where the four $PdCl_2$ units are coordinated to the pyridine N atoms of the external dipyridinopyrazine fragments ("py-py" coordination).[5] The quasi-planar peripheral $N_{2(py)}PdCl_2$ coordination sites lie nearly orthogonal to the plane of the pyrazinoporphyrazine ring, similar to what was structurally observed in the palladated precursor $[(CN)_2Py_2PyzPdCl_2]$[5a] where the $N_{2(py)}PdCl_2$ unit is orthogonal to the plane of the pyrazine ring. Although four isomers of [$(PdCl_2)_4$LPd] are theoretically possible (depending on the relative orientation of the N_2PdCl_2 fragments with respect to the pyrazinoporphyrazine plane), NMR $^1H-^1H$ COSY experiments and density functional theory (DFT) calculations both indicated[5a] that the predominant isolated isomer has the four $N_{2(py)}PdCl_2$ moieties directed on the same side of the central π-conjugated central framework (C_{4v} symmetry) as shown in Figure 1. This type of pentametallic structural arrangement is, to our knowledge, unparalleled in the literature of porphyrins, phthalocyanines, or porphyrazines.

Electrochemical studies of the triad of complexes [LPd], [L′Pd]$^{8+}$, and [$(PdCl_2)_4$LPd] showed a much easier reduction of these three compounds[5a] as compared to their phthalocyanine analogues.[4] It was also established that the Pd^{II} pyrazinoporphyrazine complexes can act as photosensitizers for the production of singlet oxygen,[5b] thus behaving as promising materials for use in photodynamic therapy (PDT), a widely expanding anticancer therapeutic modality.[6]

The present study extends our investigation to the synthesis, structure, spectroscopic, and electrochemical behavior of the pentanuclear heterometallic complexes [$(PdCl_2)_4$LM], where M = Zn^{II}, Cu^{II} Mg^{II}(H_2O). The triad of Cd^{II} complexes, that is, the mononuclear [LCd], the pentanuclear [$(PdCl_2)_4$-LCd], and the octacation [L′Cd]$^{8+}$ are also reported for the first time. The structural, physicochemical, and redox properties of these metallomacrocycles are discussed in the light of previously published data on the related mononuclear, pentanuclear, and octacationic analogues.[2,3,5]

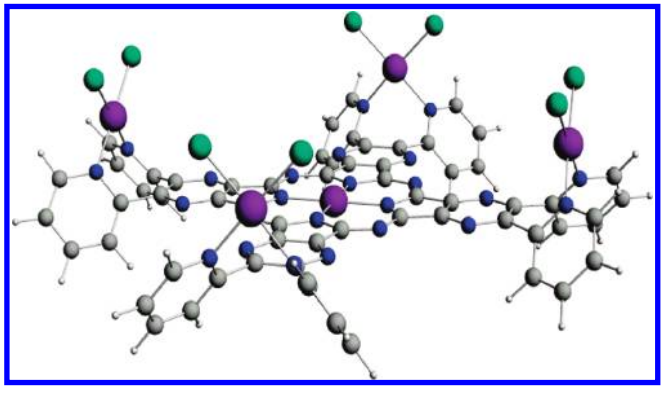

Figure 1. Predominant component present in the mixture of structural isomers of [$(PdCl_2)_4$LPd] having the four external $N_{2(py)}PdCl_2$ moieties all oriented on the same side of the central pyrazinoporphyrazine core. Adapted from ref 5a.

Experimental Section

Solvents and reagents were commercially obtained and used as received unless otherwise specified. The compounds [LM] (M = Zn^{II}, Cu^{II}, Mg^{II}(H_2O)), used as starting materials

(4) Clack, D. W.; Hush, N. S.; Woolsey, I. S. *Inorg. Chim. Acta* **1976**, *19*, 129.

(5) (a) Donzello, M. P.; Viola, E.; Xiaohui, C.; Mannina, L.; Rizzoli, C.; Ricciardi, G.; Ercolani, C.; Kadish, K. M.; Rosa, A. *Inorg. Chem.* **2008**, *47*, 3903. (b) Donzello, M. P.; Viola, E.; Bergami, C.; Dini, D.; Ercolani, C.; Giustini, M.; Kadish, K. M.; Meneghetti, M.; Monacelli, F.; Rosa, A; Ricciardi, G. *Inorg. Chem.* **2008**, *47*, 8757.

(6) (a) Redmond, R. W.; Gamlin, J. N. *Photochem. Photobiol.* **1999**, *70*, 391. (b) Szacilowski, K.; Macyk, W.; Drzewiecka-Matuszek, A.; Brindell, M.; Stochel, G. *Chem. Rev.* **2005**, *105*, 2647–2694. (c) Detty, M. R.; Gibson, S. L.; Wagner, S. J. *J. Med. Chem.* **2004**, *47*, 3897–3915. (d) De Rosa, M. C.; Crutchley, R. J. *Coord. Chem. Rev.* **2002**, *233−234*, 351–371. (e) Pandey, R. K.; Zheng, G. In *The Porphyrin Handbook*; Kadish, K. M., Smith, K. M., Guilard, R., Eds.; Academic Press: San Diego, CA, **2000**; Vol. *6*, Chapter 43, pp 157−230; (f) Dougherty, T. J.; Gomer, C. J.; Henderson, B. W.; Jori, G.; Kessel, D.; Korbelik, M.; Moan, J.; Peng, Q. *J. Natl. Cancer Inst.* **1998**, *90*, 889–905.

Scheme 2

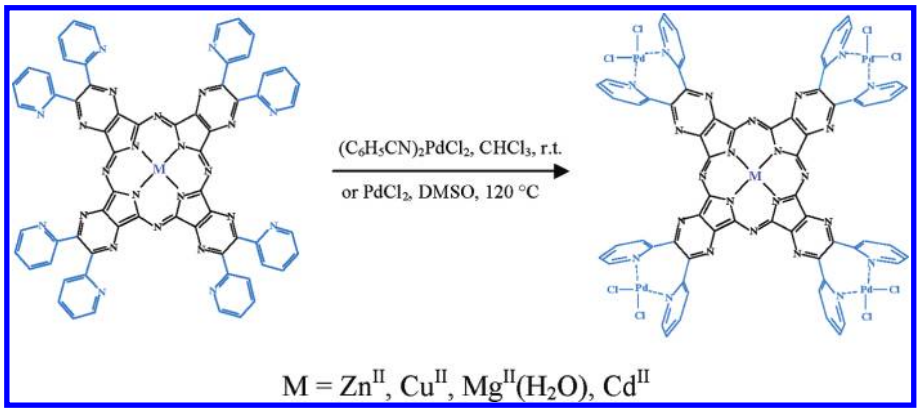

in the synthesis, were prepared as described previously.[2a] Bis(benzonitrile)palladiumdichloride, $(C_6H_5CN)_2PdCl_2$, was prepared as reported in the literature.[7] Dimethylsulfoxide (DMSO), when used in the synthesis, was freshly distilled over CaH_2 before use. Experimental details for preparation of the newly synthesized compounds are described below.

[LCd]·4H$_2$O. A suspension in pyridine (3 mL) of $[LH_2]\cdot 4H_2O$ (207 mg, 0.17 mmol) and $Cd(OAc)_2\cdot 2H_2O$ (235 mg, 0.88 mmol) was refluxed for 4 h. After cooling, the solid material was separated by centrifugation, washed repeatedly with water, and brought to constant weight under vacuum (10^{-2} mmHg) (130 mg, yield 58%). Calcd for $[LCd]\cdot 4H_2O$, $C_{64}H_{40}CdN_{24}O_4$: C, 58.17; H, 3.05; N, 25.44. Found: C, 58.35; H, 3.24; N, 24.63%. IR (KBr, cm^{-1}): 3400 w (very broad), 1632 w, 1585 m, 1566 m, 1551 w-m, 1504 vw, 1474 m, 1433 w-m, 1417 w, 1360 m, 1308 vw, 1290 vw, 1240 vs, 1190 m-s, 1148 w, 1111 m-s, 993 m, 958 m-s, 841 w, 829 w, 783 m, 744 m, 706 vs, 656 w-m, 631 vw, 611 vw, 548 w, 440 w, 405 vw.

[L′Cd](I)$_8$. $[LCd]\cdot 4H_2O$ (40 mg, 0.030 mmol) and CH_3I (0.20 mL, 3.0 mmol) was added to *N*,*N*-dimethylformamide (DMF, 1 mL), and the mixture was kept at room temperature for 22 h. After evaporation of excess CH_3I in air at room temperature, a precipitate was separated, washed with benzene and ether, and brought to constant weight under vacuum (10^{-2} mmHg) (23 mg). A second portion of the complex was isolated from the mother liquors, after addition of benzene (36 mg; total yield 50%). Calcd for [L′Cd](I)$_8$, $C_{72}H_{56}CdI_8N_{24}$: C, 36.26; H, 2.37; N, 14.09. Found: C, 37.46; H, 2.96; N, 14.98%. IR (KBr, cm^{-1}): 3450 w-m (broad), 3030 w, 3012 w, 1624 m, 1584 m, 1541 vw, 1483 vw, 1474 vw, 1435 vw, 1360 m, 1310 vw, 1240 s, 1184 m-s, 1171 m, 1148 w, 1109 w-m, 1040 vw, 995 w-m, 951 m, 839 w, 827 vw, 795 w, 770 w-m, 748 m, 698 s, 648 m, 627 vw, 600 w, 577 w, 436 w.

[(PdCl$_2$)$_4$LM]·*x*H$_2$O. The hydrated tetrapalladated $[(PdCl_2)_4$-LM] derivatives (M = Zn^{II}, Cu^{II}, Mg^{II}(H$_2$O), Cd^{II}; x = 1−14) were prepared from the related mononuclear compounds [LM] (M = Zn^{II}, Cu^{II}, Mg^{II}(H$_2$O)[2a] and [LCd], by reaction with $PdCl_2$ in DMSO or $(C_6H_5CN)_2PdCl_2$ in $CHCl_3$, under the experimental conditions illustrated in Scheme 2. It should be noted that the Mg^{II} and Cd^{II} tetrapalladated species frequently undergo transmetalation processes during preparation, leading to materials containing the pentapalladated species $[(PdCl_2)_4LPd]$ as a contaminant, the amount of which varied from minimal to significant depending on the batch preparation (see further discussion on this point below). The synthetic procedures reported below are those in which a negligible amount of contaminant was formed.

Synthesis of [(PdCl$_2$)$_4$LZn]·2H$_2$O in DMSO. $[LZn]\cdot 2H_2O$ (38 mg, 0.031 mmol) was suspended (partly dissolved) in DMSO (2 mL). After addition of $PdCl_2$ (28 mg, 0.16 mmol), the mixture was heated under stirring at 120 °C for 5 h. After cooling, the solid material was separated from the mother liquors by centrifugation, washed with water and acetone, and brought to constant weight under vacuum (10^{-2} mmHg) (55 mg, yield 91%). Calcd for $[(PdCl_2)_4LZn]\cdot 2H_2O$, $C_{64}H_{36}Cl_8N_{24}O_2Pd_4Zn$: C, 39.46; H, 1.86; N, 17.26; Pd, 21.85. Found C, 40.22; H, 2.78; N, 16.77; Pd, 20.85%. IR (cm^{-1}, KBr): 3430 w (broad), 1624 w, 1599 w-m, 1585 w-m, 1566 w, 1547 w-m, 1485 m-s, 1435 w, 1416 vw, 1360 s, 1292 w-m, 1244 vs, 1190 m-s, 1161 w, 1119 m-s, 1107 m, 1094 m, 1034 w-m, 957 s, 897 vw, 856 w-m, 829 w, 824 w, 785 m, 773 m, 746 m-s, 708 vs, 690 w-m, 656 m-s, 631 w, 617 w, 581 vw, 555 m, 525 vvw, 505 w, 496 w, 436 m, 407 w, 340 m/ν(Pd−Cl).

[(PdCl$_2$)$_4$LZn]·6H$_2$O in CHCl$_3$. $[LZn]\cdot 6H_2O$ (73 mg, 0.056 mmol) was suspended in $CHCl_3$ (20 mL) and $(C_6H_5CN)_2$-$PdCl_2$ (110 mg, 0.29 mmol) was added to the mixture which was stirred at room temperature for about 5 h. The resulting brilliant green solid material was separated by centrifugation, washed several times with $CHCl_3$, and brought to constant weight under vacuum (10^{-2} mmHg) (90 mg, yield 80%). Calcd for $[(PdCl_2)_4LZn]\cdot 6H_2O$, $C_{64}H_{44}Cl_8N_{24}O_6Pd_4Zn$: C, 38.06; H, 2.20; N, 16.64; Pd, 21.07. Found C, 38.51; H, 2.18; N, 16.32; Pd, 21.36%.

[(PdCl$_2$)$_4$LCu]·6H$_2$O in DMSO. $[LCu]\cdot 6H_2O$ (44 mg, 0.034 mmol) was suspended in DMSO (3 mL), and $PdCl_2$ (44 mg, 0.25 mmol) was added to the mixture which was stirred at 120 °C for about 5 h. The resulting green solid material was separated by centrifugation, washed with water and acetone, and brought to constant weight under vacuum (10^{-2} mmHg) (60 mg, yield 87%). Calcd for $[(PdCl_2)_4LCu]\cdot 6H_2O$, $C_{64}H_{44}Cl_8CuN_{24}O_6Pd_4$: C, 38.09; H, 2.20; N, 16.66; Pd, 21.09. Found C, 38.70; H, 3.29; N, 14.09; Pd, 22.10%. IR (cm^{-1}, KBr): 3450 m (broad), 1616 w, 1599 w-m, 1558 w-m, 1508 w, 1493 w-m, 1485 w-m, 1452 w-m, 1437 vvw, 1360 s, 1294 w, 1244 vs, 1192 m, 1161 w, 1124 s, 1092 w-m, 1061 vvw, 1034 w, 961 m, 897 vvw, 866 vw, 822 vw, 804 vw, 773 m, 750 m, 710 vs, 690 w, 656 w-m, 579 vvw, 557 w-m, 503 vw, 436 w, 340 m/ν(Pd−Cl).

[(PdCl$_2$)$_4$LCu]·12H$_2$O in CHCl$_3$. $[LCu]\cdot 6H_2O$ (24 mg, 0.018 mmol) was suspended in $CHCl_3$ (25 mL) and then $(C_6H_5CN)_2PdCl_2$ (100 mg, 0.26 mmol) was added, and the mixture was stirred at room temperature for 1 h. The solid material was separated by centrifugation, washed several times with $CHCl_3$, and brought to constant weight under vacuum (10^{-2} mmHg) (30 mg, yield 78%). Calcd for $[(PdCl_2)_4LCu]\cdot 12H_2O$, $C_{64}H_{56}Cl_8CuN_{24}O_{12}Pd_4$: C, 36.15; H, 2.65; N, 15.81. Found C, 35.91; H, 2.44; N, 15.06%.

[(PdCl$_2$)$_4$LMg(H$_2$O)]·9H$_2$O in DMSO. $[LMg(H_2O)]\cdot 7H_2O$ (67 mg, 0.051 mmol) was suspended (partly dissolved) in DMSO (4 mL). After adding $PdCl_2$ (64 mg, 0.36 mmol), the mixture was heated at 120 °C for 5 h. After cooling, a solid fraction was separated by centrifugation, washed with water and acetone,

(7) Kharasch, M. S.; Seyler, R. C.; Mayo, F. R. *J. Am. Chem. Soc.* **1938**, *60*, 882.

and brought to constant weight under vacuum (10^{-2} mmHg) (85 mg, yield 81%). Calcd for $[(PdCl_2)_4LMg(H_2O)]\cdot 9H_2O$, $C_{64}H_{52}Cl_8MgN_{24}O_{10}Pd_4$: C, 37.48; H, 2.56; N, 16.39; Pd, 20.76. Found: C, 37.64; H, 2.83; N, 15.78; Pd, 20.26%. IR (KBr, cm^{-1}): 3425 m (broad), 1625 m, 1600 s, 1550 w, 1470 s, 1380 s, 1300 w, 1250 vs, 1190 s, 1165 m, 1120 m, 1105 m, 1085 m, 1040 m, 955 s, 865 vw, 820 vw, 780 m, 750 m, 715 vs, 660 w, 570 w, 440 vw, 340 m/ν(Pd−Cl).

$[(PdCl_2)_4LMg(H_2O)]\cdot 14H_2O$ in $CHCl_3$. $[LMg(H_2O)]\cdot 5H_2O$ (412 mg, 0.32 mmol) was suspended in $CHCl_3$ (100 mL) and then $(C_6H_5CN)_2PdCl_2$ (623 mg, 1.62 mmol) was added to the mixture which was stirred at room temperature for 1 h. The solid material was separated by centrifugation, washed several times with $CHCl_3$, and brought to constant weight under vacuum (10^{-2} mmHg) (650 mg, yield: 95%). Calcd for $[(PdCl_2)_4LMg(H_2O)]\cdot 14H_2O$, $C_{64}H_{62}Cl_8MgN_{24}O_{15}Pd_4$: C, 35.90; H, 2.92; N, 15.70; Pd, 19.88. Found: C, 35.64; H, 2.05; N, 15.39; Pd, 20.80%. Thermogravimetric analysis shows a 10.8% weight loss (water) from room temperature up to 130 °C (calcd for 15 H_2O: 12.6%).

$[(PdCl_2)_4LCd]\cdot 14H_2O$ in DMSO. $[LCd]\cdot 4H_2O$ (32 mg, 0.024 mmol) was suspended (partly dissolved) in DMSO (2 mL). After addition of $PdCl_2$ (19 mg, 0.11 mmol), the mixture was heated under stirring at 120 °C for 5.5 h. After cooling, the solid material was separated from the mother liquor by centrifugation, washed abundantly with water and acetone, and brought to constant weight under vacuum (10^{-2} mmHg) (47 mg, yield 88%). Calcd for $[(PdCl_2)_4LCd]\cdot 14H_2O$, $C_{64}H_{60}CdCl_8N_{24}O_{14}Pd_4$: C, 34.77; H, 2.74; N, 15.20; Pd, 19.25 . Found: C, 34.73; H, 2.77; N, 14.37; Pd, 18.02%. IR (KBr, cm^{-1}): 3400 w (very broad), 1767 w, 1676 m, 1626 m-s, 1598 s, 1558 m-s, 1518 w, 1485 s, 1360 s, 1312 vw, 1290 vw, 1246 vvs, 1190 s, 1168 m-s, 1132 s, 1107 w, 1092 w, 1057 vw, 1022 w-m, 953 m, 893 vw, 883 vw, 841 w, 810 w, 775 s, 756 m, 714 vs, 706 s, 654 m, 629 vw, 613 vw, 559 m, 505 vw, 436 w-m; 345,340 m-s/split ν(Pd−Cl).

NMR Spectral Measurements. ^1H and ^{13}C NMR spectra were performed in DMF-d_7 solutions (99.5% DMF-d_7 CIL, 0.4 mL) at 300 K on a Bruker AVANCE AQS600 spectrometer operating at the proton frequency of 600.13 MHz and equipped with a Bruker multinuclear z-gradient inverse probehead capable of producing gradients in the z direction with a strength of 55 G cm^{-1}. The ^1H spectra were obtained using 32 K data points, a recycle delay of 8 s and a 90° flip angle pulse of 9 μs. To obtain ^1H and ^{13}C assignments, $^1H-^{13}C$ HSQC experiments were made using 512 and 1024 data points in F1 and F2 dimensions, respectively, a relaxation delay of 2 s, and a coupling constant of 150 Hz. ^1H and ^{13}C chemical shifts were referred to the residual singlet proton (8.03 ppm) and to the residual CH carbon (162.5 ppm) of DMF-d_7.

Electrochemistry. Cyclic voltammetry was performed with an EG&G Model 173 potentiostat coupled to an EG&G Model 175 Universal Programmer. Current−voltage curves were recorded on an EG&G Princeton Applied Research model R-0151 X-Y recorder. A three-electrode system was used, consisting of a glassy carbon working electrode, a platinum counter electrode, and a saturated calomel reference electrode (SCE).

UV−visible spectroelectrochemical experiments were carried out with a homemade thin-layer cell which has a light-transparent platinum gauze working electrode.[8] The applied potential was monitored with an EG&G Model 173 potentiostat, and UV−visible spectra were recorded on a Hewlett-Packard Model 8453 diode array spectrophotometer.

Three solvents were used for electrochemical measurements, pyridine (99.9+%), DMSO (99.9+%), and DMF (99.8+%). These were purchased from Sigma-Aldrich Co. and used without further purification. High purity N_2 from Trigas was used to deoxygenate the solution before each electrochemical and spectroelectrochemical experiment. Tetra-*n*-butylammonium perchlorate (TBAP, 99%) from Fluka Chemika Co. was used as supporting electrolyte (0.1 M for cyclic voltammetry and 0.2 M for spectroelectrochemistry) and stored under vacuum at 40 °C prior to use.

Other Physical Measurements. IR spectra were recorded on a Perkin-Elmer 783 instrument in the range 4000−200 cm^{-1} (KBr pellets). UV−visible solution spectra, other than those for spectroelectrochemistry (see above) were recorded with a Varian Cary 5E spectrometer. Thermogravimetric analyses (TGA) were performed on a Stanton Redcroft model STA-781 analyzer under a N_2 atmosphere (0.5 L/min). Elemental analyses for C, H, and N were provided by the "Servizio di Microanalisi" at the Dipartimento di Chimica, Università "La Sapienza" (Rome) on an EA 1110 CHNS-O instrument. The ICP-PLASMA Pd analyses were performed on a Varian Vista MPX CCD simultaneous ICP-OES.

Results and Discussion

Synthesis, IR and UV−visible Spectral Features. As described in the Experimental Section, all of the reported compounds carry clathrated water molecules, the amount of which varied from batch to batch for each compound. With the exception of Table 1, the presence of hydrated water molecules is not shown in further notation for the compounds. The $[(PdCl_2)_4LM]$ complexes where M = Zn^{II}, Cu^{II}, $Mg^{II}(H_2O)$ were obtained by palladation of the previously characterized mononuclear [LM] derivatives.[2a] The Cd^{II} complexes [LCd], the pentanuclear $[(PdCl_2)_4LCd]$, and the salt-like species $[L'Cd](I_8)$ were synthesized as new compounds in the present study, and their properties are described below.

Figure 2 shows IR spectra of the three Cd^{II} complexes in the 1800−400 cm^{-1} region. As can be seen, an IR band is observed for [LCd] at 993 cm^{-1} (Figure 2-A). This absorption compares to a band at 993/994 cm^{-1} seen for all previously characterized [LM] derivatives[2a] and is not observed for any of the $[(PdCl_2)_4LM]$ complexes, including $[(PdCl_2)_4LCd]$ whose spectrum is shown in Figure 2-B. A second absorption, also typical of [LM], is seen for [LCd] at 958 cm^{-1}. The position of this absorption varies with the central metal ion of the macrocycle as earlier reported,[2a,5a] that is, 956/Mg^{II}, 966/Mn^{II}, 971/Co^{II}, 964/Cu^{II}, 954/Zn^{II}, and 972/Pd^{II}. This absorption is still present in the related pentanuclear species $[(PdCl_2)_4LM]$ and shows only a minimal change of position (3−5 cm^{-1}; see Figure 2-B for Cd^{II}). A ν(Pd−Cl) absorption is also present at about 350 cm^{-1} for the tetrapalladated species. Similar to [LCd], $[L'Cd]^{8+}$ also exhibits two peaks in the region 950−1000 cm^{-1} (Figure 2-C); there are also absorptions assigned to the methyl groups of the octacation seen at 3000−3100 cm^{-1} (not reported).

Table 1 compares UV−visible spectra for the four metalated triads of compounds [LM], $[(PdCl_2)_4LM]$, and $[L'M]^{8+}$ in DMSO and DMF containing 0.2 M TBAP which was used as supporting electrolyte in the electrochemical experiments. Spectral data cannot be presented in pyridine since all of the pentanuclear complexes are unstable in this solvent and lose $PdCl_2$ with formation of [LM] as previously described for $[(PdCl_2)_4LPd]$.[5a] A dissociation of $PdCl_2$ is not observed for any of the currently investigated pentanuclear complexes in DMSO or DMF, and clear spectral differences for [LM], $[(PdCl_2)_4LM]$, and $[L'M]^{8+}$ can be observed as seen in Table 1.

(8) Lin, X. Q.; Kadish, K. M. *Anal. Chem.* **1985**, *57*, 1489.

The spectra of all compounds are characterized by the presence of an intense Q band at 648−674 nm, a Soret band at 360−379 nm, plus vibrational bands in the region 590−610 nm. After external palladation or quaternization of [LM] at the dipyridinopyrazine fragments, the Q bands of the resulting $[(PdCl_2)_4LM]$ or $[L'M]^{8+}$ products are in each case shifted bathochromically as compared to the [LM] derivatives with the same central metal ion (Table 1).[3b,5a] This is evidently the result of a lowering of the HOMO−LUMO gap upon going from [LM] to $[(PdCl_2)_4LM]$ or [LM] to $[L'M]^{8+}$, and these spectral results parallel what is seen in the electrochemical data described in a later section of the manuscript.

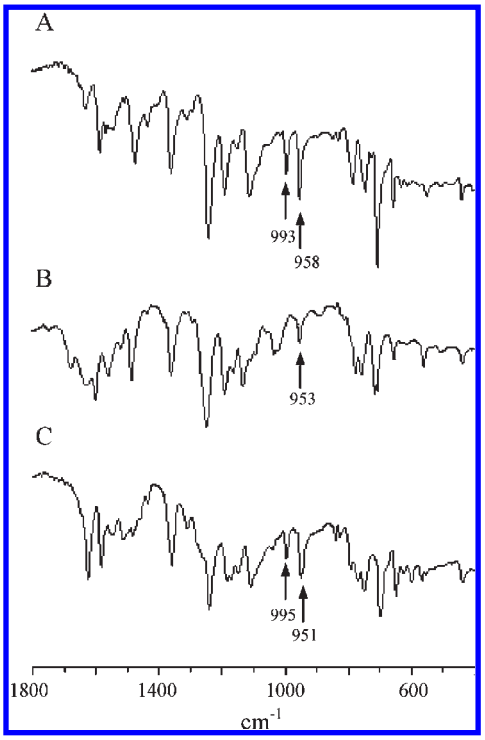

Figure 2. IR spectra (KBr pellets) of (A) [LCd], (B) $[(PdCl_2)_4LCd]$ and (C) $[L'Cd](I_8)$ in the range 1800−400 cm^{-1}.

^{1}H and ^{13}C NMR Measurements. Previous single-crystal X-ray work on the complexes $[(CN)_2Py_2PyzPdCl_2]$[5a] and $[(CN)_2Py_2PyzPtCl_2]$,[9] obtained by metalation with $PdCl_2$ and, respectively, $PtCl_2$ of 2,3-dicyano-5,6-di(2-pyridyl)pyrazine, $[CN)_2Py_2Pyz]$, provided useful information about the "py-py" coordination of the metal centers to the dipyridinopyrazine fragment (see Supporting Information, Figure S1 for the Pd^{II} complex); in addition, the $N_{2(py)}Pd/PtCl_2$ square planar coordination site lies almost orthogonal to the plane of the pyrazine ring. Assuming the same structural arrangement for the dipyridinopyrazine-$PdCl_2$ moiety of the currently examined heteropentametallic macrocycles, four isomers would be predicted (see Supporting Information, Scheme S1). This aspect was previously discussed for the homopentanuclear complex $[(PdCl_2)_4LPd]$ on the basis of experimental ^{1}H NMR data (^{1}H−^{1}H COSY experiments) and theoretical DFT calculations. NMR data were suggesting the presence of one predominant isomer.[5a] The computed solvation energy for the synthesis of the compound in DMSO indicated that the stabilization energy in this solvent was considerably higher for the 4:0 form (C_{4v} symmetry; Supporting Information, Scheme S1 and Figure 1) than those measured for the 2:2-*cis* (C_i symmetry) or 2:2-*trans* (D_{2d} symmetry) forms by 89.0 and 119.7 kJ mol^{-1}, respectively, and therefore the 4:0 form was indicated as the predominant isomer. NMR data in the earlier study[5a] also indicated the presence of a small amount of a minority isomer, assigned either as 2:2-cis or 2:2-trans which were not differentiated. The 3:1 isomer was excluded as a possibility because of an incompatibility of the NMR spectrum with symmetry requirements.

NMR spectral data indicate that the above structural organization (4:0 form; see Figure 1) is also present for the Zn^{II} tetrapalladated species $[(PdCl_2)_4LZn]$ examined in

Table 1. UV-Visible Spectral Data (λ, nm) of the Compounds [LM], $[(PdCl_2)_4LM]$, and $[L'M](I_8)$ in DMSO, and DMF (0.2 M TBAP)

		λ (nm) (log ε)			
solvent	compound[a]	Soret region	Q-band region		ref[b]
DMSO	$[LZn]\cdot 5H_2O$	372 (5.10)	592 (4.54)	655 (5.36)	3b
	$[(PdCl_2)_4LZn]\cdot 6H_2O$	378 (4.60)	600 (4.18)	664 (4.88)	tw
	$[L'Zn](I_8)\cdot 2H_2O$	373 (4.37)	600 (3.86) (sh)	666 (4.74)	3b
	$[LCu]\cdot H_2O$	365 (4.91)	590 (4.44)	648 (5.18)	3b
	$[(PdCl_2)_4LCu]\cdot 12H_2O$	379 (4.76)	604 (4.29)	665 (4.94)	tw
	$[L'Cu](I_8)\cdot 4H_2O$	359 (4.95)	593 (4.46)	655 (5.18)	3b
	$[LCd]\cdot 4H_2O$	368 (5.29)	600 (4.68)	666 (5.26)	tw
	$[(PdCl_2)_4LCd]\cdot 14H_2O$	374 (4.81)	604 (4.64)	674 (5.03)	tw
	$[L'Cd](I_8)$	360 (5.19)	608 (4.73)	671(5.02)	tw
	$[LMg(H_2O)]\cdot 4H_2O$	374 (5.08)	594 (4.36)	653 (5.34)	3b
	$[(PdCl_2)_4LMg(H_2O)]\cdot 14H_2O$	360 (5.19)	603 (4.66)	660 (5.29)	tw
	$[L'Mg(H_2O)](I_8)\cdot 5H_2O$	370 (4.83)	600 (4.33)	660 (5.15)	3b
DMF	$[LCd]\cdot 4H_2O$	373 (5.30)	600 (4.72)	663 (5.47)	tw
	$[(PdCl_2)_4LCd]\cdot 14H_2O$	373 (4.54)	605 (4.11)	672 (4.88)	tw
	$[L'Cd](I_8)$	362 (5.17)	609 (4.68)	671 (5.04)	tw
	$[(PdCl_2)_4LMg(H_2O)]\cdot 14H_2O$	368 (5.20)	603 (4.81)	662 (5.40)	tw
	$[(PdCl_2)_4LCu]\cdot 12H_2O$	370 (4.63)	604 (4.15)	668 (4.85)	tw
	$[(PdCl_2)_4LZn]\cdot 6H_2O$	379 (4.66)	603 (4.21)	662 (4.96)	tw

[a]Clathrated water specified for the batch used for measuring the spectra. [b]tw = this work.

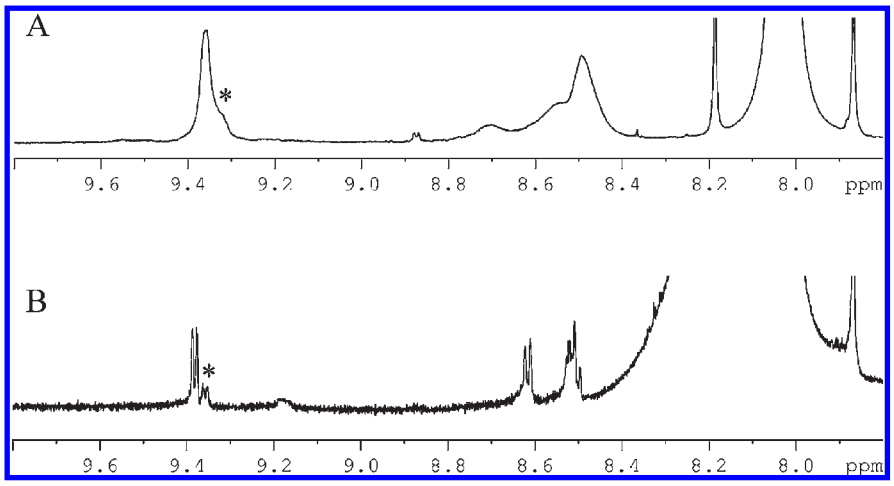

Figure 3. ^{1}H NMR spectra in DMF-d_7 at 300 K of (A) [$(PdCl_2)_4$LZn] and (B) [$(PdCl_2)_4$LPd] (adapted from ref 5a), both synthesized in DMSO.

Table 2. ^{1}H and ^{13}C NMR Spectral Data Taken at 300 K in DMF-d_7 for the Pentanuclear Complexes [$(PdCl_2)_4$LM] (M = Zn^{II}, Pd^{II}) Synthesized in DMSO (* = Minor Component)

	[$(PdCl_2)_4$LZn][a]		[$(PdCl_2)_4$LPd][a]
	^{1}H (ppm)	^{13}C (ppm)	^{1}H (ppm)
α	9.36	153.2	9.382
	9.32*		9.357*
β	8.02[b]	127.1	8.047
			8.051*
γ	8.49	141.1	8.507
			8.514*
δ	8.7	130.0	8.615

[a]Solvent used for the synthesis: DMSO. [b]The assignment of the hidden β proton was obtained by means of ^{1}H−^{13}C HSQC experiments.

the present study. The ^{1}H NMR spectra in DMF-d_7 of this complex and the related Pd^{II} analogue [$(PdCl_2)_4$LPd] (both prepared in DMSO) are shown in Figure 3. A summary of the ^{1}H and ^{13}C NMR chemical shifts are given in Table 2. Although the spectrum of [$(PdCl_2)_4$LZn] (Figure 3-A) is clearly less resolved than that of [$(PdCl_2)_4$LPd] (Figure 3-B),[5a] the positions of the proton resonance peaks for the two species are quite similar to each other (see exact values in Table 2). As to the Zn^{II} complex, the identification of the NMR signals made by the ^{1}H−^{13}C HSQC experiment allows unequivocal assignment of the α, β, and γ protons at 9.36, 8.02, and 8.49 ppm, respectively. Only for the δ proton peak resonance at 8.7 ppm (^{13}C at 130 ppm) assignment in the spectrum (Figure 3-A) appears less clear, very likely peak position and relative intensity of the peak being influenced by signal broadening. Despite of this, the overall features of the ^{1}H NMR spectrum leads to the conclusion that the predominant isomeric form for the Zn^{II} compound is 4:0 (C_{4v} symmetry, Supporting Information, Scheme S1 and Figure 1), as was previously established for the Pd^{II} complex (see discussion above).

As can also be seen in Figure 3-A (data in Table 2) the spectrum of [$(PdCl_2)_4$LZn] shows a peak at 9.32 ppm (*) on the tail of the peak at 9.36 ppm. This unresolved peak can be compared to a small doublet at 9.357 ppm in the spectrum of [$(PdCl_2)_4$LPd][5a] (Figure 3-B and Table 2) and assigned as due to a minor component present in mixture with the more abundant isomer. This minor component was assigned as a 2:2-*cis* or 2:2-*trans* isomer in the case of [$(PdCl_2)_4$LPd][5a], and the same minor isomeric form is proposed to exist in the sample of [$(PdCl_2)_4$LZn]. The observed NMR data on this complex and on [$(PdCl_2)_4$LPd] seem to indicate that the 4:0 isomer is the prevalent component formed in DMSO, no matter which the central metal ion (Zn^{II}, Pd^{II}). NMR data on the related Mg^{II} and Cd^{II} complexes (see below) give further support to these findings. Noticeably, the structure in Figure 1, where the four exocyclic metal centers are displaced out-of-plane is, to our knowledge, quite a rare occurrence (if not unique) in the context of pentametallic macrocyclic systems where five metal centers are generally found to be distributed in a coplanar fashion.[10]

The combined spectral data (IR, UV−visible, and NMR), as well as the electrochemical data described later in the paper, are self-consistent in indicating that the synthetic procedures of the Mg^{II} and Cd^{II} tetrapalladated species suffer often from complications because of the concomitant transmetalation processes of the type [$LMg(H_2O)$] → [$(PdCl_2)_4$LPd] and [LCd] → [$(PdCl_2)_4$LPd], with a consequent formation of the pentapalladated product as a contaminant. From a general viewpoint, transmetalation processes involving Mg^{II} or Cd^{II} are frequently observed with porphyrazines and porphyrins. Examples were earlier reported for the unsubstituted tetraazaporphine,[11] and for the tetrakis(thiadiazole)-porphyrazinato-copper(II) derivative, [TTDPzCu], which could be prepared from the corresponding Mg^{II} complex by reaction with $Cu(OCOCH_3)_2 \cdot H_2O$.[12] A similar process led to the preparation of Zn^{II} and Pd^{II} bacteriochlorophyll *a* (BChl) complexes from Cd-BChl,[13] which was also used for synthesis of a more extended number of BChl metal derivatives[14] and include Cd^{II} porphyrins

(9) Cai, X.; Donzello, M. P.; Rizzoli, C.; Ercolani, C.; Kadish, K. M. *Inorg. Chem.* **2009**, *48*, 9890.

(10) See for example: Michel, S. L. J.; Hoffman, B. M.; Baum, S. M.; Barrett, A. G. M. *Progress in inorganic chemistry*; Carli, K. D., Ed.; John Wiley & Sons, Inc: New York, 2001; pp 475−590.

(11) Ficken, G. E.; Linstead, R. P. *J. Chem. Soc.* **1952**, 4846.

(12) Stuzhin, P. A.; Bauer, E. M.; Ercolani, C. *Inorg. Chem.* **1998**, *37*, 1533.

(13) Musewald, C.; Hartwich, G.; Pöllinger-Dammer, F.; Lossau, H.; Scheer, H.; Michel-Beyerle, M. E. *J. Phys. Chem. B* **1998**, *102*, 8336.

(14) Hartwich, G.; Fiedor, L.; Simonin, I.; Cmiel, E.; Schäfer, W.; Noy, D.; Scherz, A.; Scheer, H. *J. Am. Chem. Soc.* **1998**, *120*, 3675.

Table 3. ^{1}H NMR Spectral Data Taken at 300 K in DMF-d_7 for the Pentanuclear Complexes [$(PdCl_2)_4$LM] (M = $Mg^{II}(H_2O)$], Cd^{II}) with Resonance Peaks Given Also for the Contaminant [$(PdCl_2)_4$LPd]

	^{1}H (ppm)		
	[$(PdCl_2)_4$LMg(H_2O)]	[$(PdCl_2)_4$LCd][b]	[$(PdCl_2)_4$LCd]
α	9.36	9.34 (153.2)	9.34
β	hidden	8.01 (126.9)	hidden
γ	8.49	8.48 (141.1)	(8.47)[c]
δ	8.58	8.65 (129.9)	(8.60)[c]
	[$(PdCl_2)_4$LPd] (contaminant)		
α	9.38	9.38	9.38
β	hidden[a]	8.1	hidden[a]
γ	8.51	8.4	8.50
δ	8.62	8.6	8.62

[a]Peak at 8.047 ppm (see ref 5a). [b]The ^{1}H and ^{13}C assignments were obtained by ^{1}H−^{13}C HSQC experiment. ^{13}C carbon data in ppm are reported in brackets. [c]Tentative assignments.

in a recent work.[15] Evidence for the formation of [$(PdCl_2)_4$LPd] as side product in the present Mg^{II} and Cd^{II} compounds is given by IR spectra which show a peak typical of the pentapalladated species at 972 cm^{-1} in addition to the expected band at 955 or 953 cm^{-1} for the genuine [$(PdCl_2)_4$LMg(H_2O)] and [$(PdCl_2)_4$LCd] complexes, respectively. The transmetalation contamination product is also observed in the UV−visible spectrum of the two complexes and identified by a Q band at 636/8 nm in DMSO in addition to the major Q band at 660 (Mg^{II}) or 674 nm (Cd^{II}) (Table 1).

Despite the transmetalation side reaction, the synthetic procedures described in the present paper (Experimental Section) are those where the desired Mg^{II} and Cd^{II} heterometallic compounds were found to be contaminated by only negligible amounts of the pentapalladated species. However, it should be noted that under the same experimental conditions, different amounts of the contaminant were formed in a given synthesis depending upon the batch. The intriguing aspect concerning the formation of the pentapalladated complex as a contaminant is exemplified by ^{1}H NMR spectra reported below for samples of the Mg^{II} and Cd^{II} compounds in DMF-d_7. These data are summarized in Table 3, and the NMR spectra are shown in Figure 4 which also includes the related UV−visible spectra as insets.

The ^{1}H NMR spectrum of a sample of the Mg^{II} species [$(PdCl_2)_4$LMg(H_2O)] prepared in DMSO indicates (Figure 4-A) the presence of an isomeric form of the complex with the α proton resonance peak at 9.36 ppm (Table 3). There are also peaks at 8.49 and 8.58 ppm for the *γ* and *δ* protons of the pyridine rings of the same species (the *β* proton resonance is hidden and hence not detectable). These data closely approach those of the Zn^{II} and Pd^{II} analogues (Table 2), suggesting again that, among the four possible isomeric forms, the prevalent component in [$(PdCl_2)_4$LMg(H_2O)] is the 4:0 isomer (Figure 1). Peaks of the contaminant are listed in Table 3. The inset in Figure 4-A shows the UV−visible spectrum in DMF which confirms large prevalence of the Mg^{II} complex (Q band at 665) and only minimal presence of the contaminant (Q band at 638 nm).

(15) Shukhto, O. V.; Berezin, D. B. *J. Porphyrins Phthalocyanines* **2008**, *12*, 719.

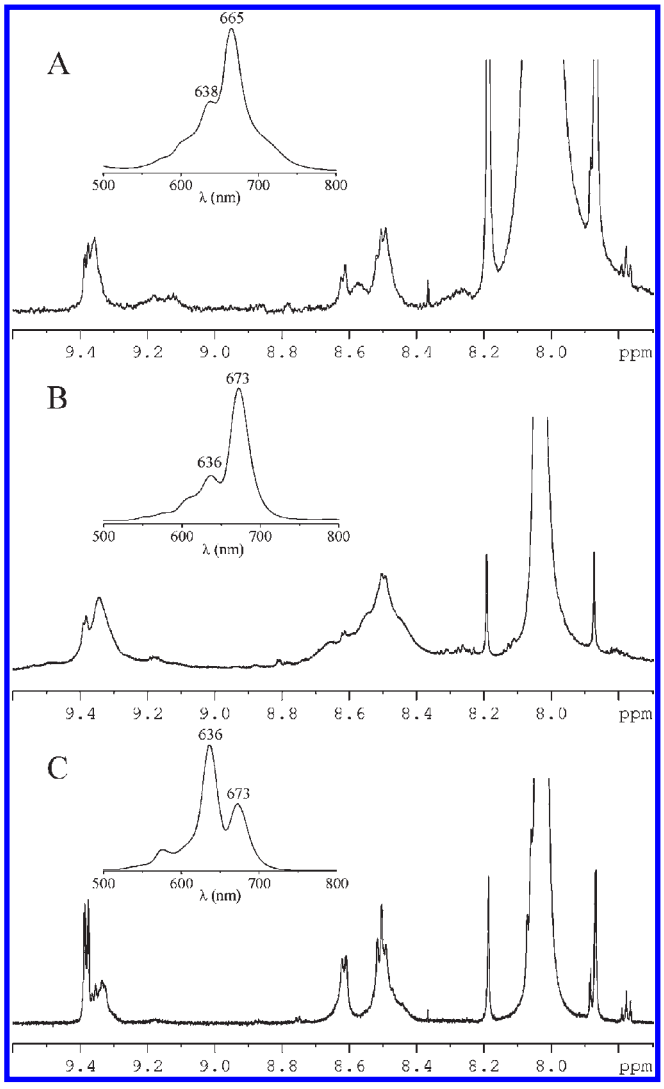

Figure 4. ^{1}H NMR spectra in DMF-d_7 at 300 K of (A) [$(PdCl_2)_4$LMg(H_2O)] and (B) [$(PdCl_2)_4$LCd] with minor contamination by the presence of the pentapalladated [$(PdCl_2)_4$LPd] and (C) [$(PdCl_2)_4$LCd] with major contamination by the presence of the pentapalladated [$(PdCl_2)_4$LPd]. The insets in the figure show the corresponding UV−visible spectra in DMF.

Figures 4-B,C show ^{1}H NMR spectra for two samples of the Cd^{II} complex prepared in DMSO, where in one of these only a minor amount of the pentapalladated compound is present (Figure 4-B). The proton resonance peaks at 9.34, 8.01, 8.48, and 8.65 ppm (Table 3) are easily detectable and assigned to the α, *β*, *γ*, *δ* protons, respectively. This once again indicates a 4:0 isomer (assignment made unequivocal by ^{1}H−^{13}C HSQC experiment). In the other sample (Figure 4-C) the contaminant is instead definitely prevalent, because of extensive transmetalation, and this is indicated by the well-resolved resonance peaks at 9.38 (α), 8.50 (*γ*) and 8.62 (*δ*) (Table 3), whereas only the α proton resonance peak at 9.34 ppm is unequivocally identified as belonging to [$(PdCl_2)_4$LCd], and is accompanied by peaks at 8.47 and 8.60 ppm for the *γ* and *δ* protons, only tentatively assigned (Table 3, data in parentheses). As shown by the related UV−visible spectra in DMF (insets of Figure 4-B,C), there is a detectable Q-band absorbance at 636 nm in the inset of Figure 4-B, assigned to a minor

Table 4. Half-Wave Potentials ($E_{1/2}$, V vs SCE) in DMSO and DMF, Containing 0.1 M TBAP

		macrocycle							
solvent	compound	1st	2nd	3rd	4th	$PdCl_2$	Δ_1[b]	Δ_2[c]	ref[d]
DMSO	$PdCl_2$					−0.86			5a
	[LZn]	−0.26	−0.67	−1.38	−1.64				3b
	$[(PdCl_2)_4LZn]$	−0.13	−0.54	−1.39	−1.63	−1.03	0.13	0.13	tw
	$[L'Zn]^{8+}$	−0.10	−0.44	−0.81	−1.24		0.16	0.23	3b
	[LCu]	−0.22	−0.58	−1.22	−1.58				3b
	$[(PdCl_2)_4LCu]$	−0.03	−0.41	−1.24	−1.60	−0.93	0.19	0.17	tw
	$[L'Cu]^{8+}$	−0.04	−0.38	−0.85	−1.22		0.18	0.20	3b
	[LCd]	−0.46	−0.79						tw
	$[(PdCl_2)_4LCd]$	−0.22	*a*	*a*	*a*	−0.98	0.24		tw
	$[L'Cd]^{8+}$	0.11	−0.32				0.57	0.47	tw
	$[LMg(H_2O)]$	−0.33	−0.70	−1.39	−1.70				3b
	$[(PdCl_2)_4LMg(H_2O)]$	−0.15	*a*	*a*	*a*	−1.00	0.18		tw
	$[L'Mg(H_2O)]^{8+}$	−0.19	−0.47	−0.84	−1.28		0.14	0.23	3b
	[LPd]	−0.26	−0.60	−1.26	−1.61				5a
	$[(PdCl_2)_4LPd]$	0.00	−0.37	−1.24	−1.59	−0.98	0.26	0.23	5a
	$[L'Pd]^{8+}$	0.08	−0.33				0.34	0.27	5a
DMF	$PdCl_2$					−0.86			5a
	$[(PdCl_2)_4LCd]$	−0.20	*a*	*a*	*a*	−1.00			tw
	$[(PdCl_2)_4LMg(H_2O)]$	−0.15	*a*	*a*	*a*	−1.06			tw
	$[(PdCl_2)_4LZn]$	−0.12	−0.52	−1.39	−1.62	−1.00			tw
	$[(PdCl_2)_4LCu]$	0.00	−0.43	−1.27	−1.62	−1.02			tw
	$[(PdCl_2)_4LPd]$	0.04	−0.37	−1.27	−1.62	−1.03			5a

[a] Complicated current−voltage curves due to overlapping peaks assigned to the pentapalladated complex present as a transmetalation contaminant (see Text). [b] Δ_1 = difference in $E_{1/2}$ between first reduction of [LM] and $[(PdCl_2)_4LM]$ or [LM] and $[L'M]^{8+}$. [c] Δ_2 = difference in $E_{1/2}$ between second reduction of [LM] and $[(PdCl_2)_4LM]$ or [LM] and $[L'M]^{8+}$. [d] tw = this work.

pentapalladated contaminant. This may be compared to the peak at 673 nm for the prevalent Cd^{II} complex, but in Figure 4-C the same absorption (636 nm) of the contaminant is clearly higher in intensity than that of the Cd^{II} species (673 nm), in agreement with the NMR data.

Thus, the synthesized samples of the Mg^{II} and Cd^{II} tetrapalladated complexes, despite of the disturbing presence of the contaminant, show NMR data which indicates that the 4:0 isomer is largely prevalent, in keeping with the results discussed above for the Zn^{II} and Pd^{II} analogues. It is therefore concluded that sufficient information has been achieved for assuming that the proposed structure in Figure 1 is that for the predominant material formed in DMSO, independent of the central metal ion.

Finally, it may be further noted that less clearly resolved ^{1}H NMR spectra are features common to the Zn^{II}, Mg^{II}, and Cd^{II} derivatives whereas the pentapalladated complex $[(PdCl_2)_4LPd]$, which is formed as a side product in mixture with Mg^{II}, and Cd^{II}, displays good NMR signal resolution (see for Cd^{II} Figure 4-B,C). This excludes the presence of paramagnetic contaminants as responsible for signal broadening. The presence of aggregation can also not be evoked to explain poor resolution of the ^{1}H NMR spectra, since UV−visible spectra clearly indicate the presence of practically pure monomeric species (Figure 4-B,C-insets; see also spectroelectrochemical data discussed below).

Electrochemistry. Cyclic voltammetry and spectroelectrochemistry of the newly synthesized compounds were carried out in three different nonaqueous solvents (pyridine, DMSO, and DMF) containing 0.1 M TBAP. The half wave potentials ($E_{1/2}$, V vs SCE) for reductions in DMSO and DMF are listed in Table 4 which also includes published data on related [LM] and $[L'M]^{8+}$ derivatives.[3b,5a] The electrochemical data is not summarized in pyridine since for the present heterometallic compounds dissociation of the four bound $PdCl_2$ groups occurs immediately upon dissolution in this solvent giving a mixture of $(py)_2PdCl_2$ and [LM] in solution, as described in a previous publication for $[(PdCl_2)_4LPd]$.[5a]

No oxidations are observed for any of the examined tetrapalladated compounds within the solvent potential window as was previously noted for related [LM], $[(PdCl_2)_4LPd]$, or $[L'M]^{8+}$ derivatives,[3b,5a] At the concentrations used for the electrochemical experiments (ca. 5×10^{-4} M or higher), the pentametallic derivatives are all soluble and present in a monomeric form as indicated by UV−visible data (narrow Q band; spectroelectrochemical data in Figures 6 and Supporting Information, Figure S3), in line with findings for the homometallic Pd^{II} analogue, $[(PdCl_2)_4LPd]$.[5a] The absence of aggregation is due most probably to steric hindrance of the four external $N_{2(py)}PdCl_2$ moieties on one side of the pyrazinoporphyrazine plane and the rigidly positioned pyridine rings on the other (Figure 1). Results of the electrochemical studies are discussed first in DMSO where comparisons are made between the redox behavior of [LM], $[(PdCl_2)_4LM]$, and $[L'M]^{8+}$ and then in DMF where behavior of the five $[(PdCl_2)_4LM]$ compounds is analyzed as a function of the central metal ion.

Cyclic voltammograms showing the reduction of $[(PdCl_2)_4LM]$ and [LM] are illustrated in Figure 5 for M = Zn^{II} and in Supporting Information, Figure S2 for M = Cu^{II}. The first two reductions of each compound involve the porphyrazine macrocycle to give a π-anion radical and dianion, respectively. The investigated compounds containing

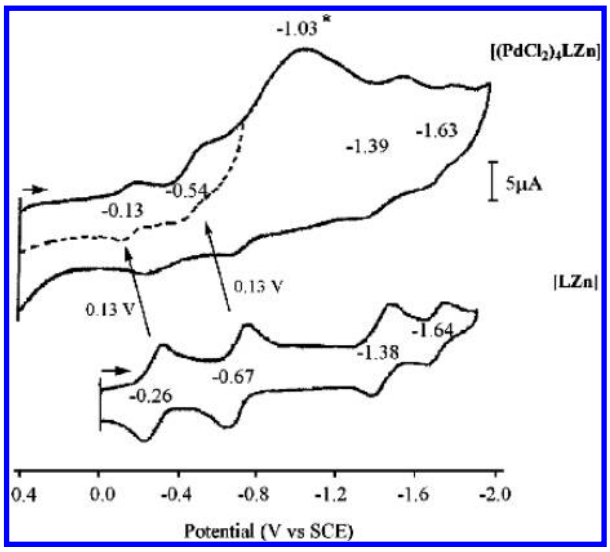

Figure 5. Cyclic voltammograms of $[(PdCl_2)_4LZn]$ and [LZn] (reproduced from ref 3b) in DMSO, 0.1 M TBAP. The peak marked by an asterisk is associated with reduction of bound $PdCl_2$.

four externally bound $PdCl_2$ units are in each case easier to reduce than the monometallic derivatives with the same central metal ion, the $E_{1/2}$ values for the first two reductions being shifted positively by 130 mV for $[(PdCl_2)_4LZn]$ (Figure 5) and 170−190 mV for $[(PdCl_2)_4LCu]$ (Supporting Information, Figure S2).

The first two one-electron additions to $[(PdCl_2)_4LM]$ are given by eqs 1 and 2 and are followed by reduction of the four bound $PdCl_2$ units at $E_p = -1.03$ V (M = Zn^{II}) or −0.93 V (M = Cu^{II}). These peak potentials can be compared to an $E_p = -0.86$ V for reduction of just $PdCl_2$ in DMSO, 0.1 M TBAP at a scan rate of 0.1 V/s.[5a]

$$[(PdCl_2)_4Py_8TPyzPzM] + e \rightleftharpoons [(PdCl_2)_4Py_8TPyzPzM]^- \quad (1)$$

$$[(PdCl_2)_4Py_8TPyzPzM]^- + e \rightleftharpoons [(PdCl_2)_4Py_8TPyzPzM]^{2-} \quad (2)$$

The 70−170 mV difference in peak potentials between E_p for reduction of bound $PdCl_2$ in the five $[(PdCl_2)_4LM]$ complexes and free $PdCl_2$ under the same solution conditions is consistent with coordination of the Pd^{II} unit at the external pyridine rings of the porphyrazine macrocycle which leads to a more negative reduction potential for this redox active species. It should also be noted that the negative shift in $E_{1/2}$ for reduction of the coordinated $PdCl_2$ group is consistent with the positive shift in $E_{1/2}$ for the first two reductions of the porphyrazine-centered reductions of $[(PdCl_2)_4LM]$, thus indicating a redistribution of negative charge density toward the $PdCl_2$ groups and away from the porphyrazine π ring system. Quite similar behavior and conclusions are observed from electrochemical data of the five $[(PdCl_2)_4LM]$ complexes in DMF (Table 4).

Two reversible and well-separated one-electron reductions are seen after reductive removal of $PdCl_2$, and the $E_{1/2}$ values for these processes are identical within experimental error to half wave potentials for the third and fourth reductions of [LZn] and [LCu] (see Table 4). This gives further evidence for a reductive loss of the bound $PdCl_2$ groups and formation of $[LZn]^{2-}$ and $[LCu]^{2-}$ at the electrode surface, as previously described for $[(PdCl_2)_4LPd]$.[5a]

Similar electrochemical reduction mechanisms are seen for the other pentametallic compounds but the current−voltage curves for $[(PdCl_2)_4LCd]$ and $[(PdCl_2)_4LMg(H_2O)]$ are ill-defined in DMSO because of overlapping reductions of the transmetalated $[(PdCl_2)_4LPd]$ species whose formation is described earlier in the manuscript. Nonetheless, the first one-electron reductions of the Cd^{II} and Mg^{II} derivatives can be easily monitored and are located at $E_{1/2} = -0.22$ and −0.15 V, respectively. These potentials are more positive than $E_{1/2}$ values for the first reductions of [LCd] and $[LMg(H_2O)]$, the magnitude of the shift being 0.24 V in the case of Cd^{II} and 0.18 V for M = Mg^{II}. The shift in potentials are given in Table 4 and listed as Δ_1 which is defined as the difference in $E_{1/2}$ between first reduction of [LM] and $[(PdCl_2)_4LM]$ or [LM] and $[L'M]^{8+}$.

In a previous study,[5a] it was pointed out that the octacationic complex $[L'Pd]^{8+}$ is easier to reduce than $[(PdCl_2)_4LPd]$, with the ease of reduction for the three compounds being [LPd] < $[(PdCl_2)_4LPd]$ < $[L'Pd]^{8+}$. The same trend in ease of reduction is seen in Table 4 for the Cd^{II} and Zn^{II} derivatives but not for the Cu^{II} and Mg^{II} complexes where the pentametallic species is slightly easier to reduce than the octacationic complexes.

In summary, the electrochemical data indicates that the first and second reductions of $[(PdCl_2)_4LM]$ are systematically easier by 130 to 240 mV than the first and second reductions of [LM] with the same central metal ion. These values are comparable with a potential difference earlier reported between $[(PdCl_2)_4LPd]$ and [LPd] (260 mV)[5a] which demonstrates that external coordination of the $PdCl_2$ units induces in all cases an easier acceptance of excess negative charge within the macrocyclic framework, independent of the central metal atom. This is in strict accordance with the enhanced electron-withdrawing properties of the external dipyridinopyrazine fragments once they are metalated. Despite the narrow range of total potential variation in $E_{1/2}$ for the first reductions in DMSO (220 mV), there is a systematic shift of the $E_{1/2}$ values toward less negative potentials over the whole series of $[(PdCl_2)_4LM]$ compounds with a more facile reduction occurring in the sequence: Cd^{II} (−0.22 V) → Mg^{II} (−0.15 V) → Zn^{II} (−0.13) → Cu^{II} (−0.03 V) → Pd^{II} (0.00 V). The same sequence holds in DMF: Cd^{II} (−0.20) → Mg^{II} (−0.15 V) → Zn^{II} (−0.12 V) → Cu^{II} (0.00 V) → Pd^{II} (0.04 V). A plausible explanation for this trend is that in the central $Pd-N_4$ bond system there is a high combination of σ and Pd(dπ)-N(pπ) interaction whereas in the $Cd-N_4$ and $Mg-N_4$ bonded systems there is a significant presence of ionic character. From this, it can be derived that more negative charge resides on the macrocycles of the Cd^{II} and Mg^{II} compounds which would make them less easily reducible. Noticeably, the same trend of half wave potentials for the first and second reductions is observed for the mononuclear compounds, [LM] (Table 4).

Short Comments on the Spectroelectrochemical Changes in Pyridine and DMSO. Figure 6 shows the UV−visible spectral changes in DMSO and pyridine during first one-electron reduction of $[(PdCl_2)_4LZn]$ and similar changes are obtained for $[(PdCl_2)_4LCu]$ (Supporting Information,

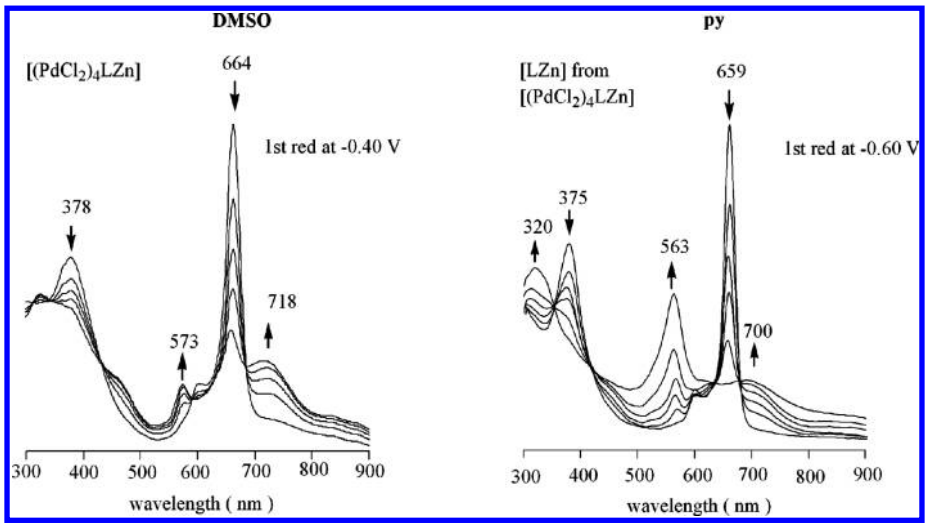

Figure 6. UV−visible spectral changes during the first one-electron reduction of $[(PdCl_2)_4LZn]$ in DMSO and [LZn] (formed from $[(PdCl_2)_4LZn]$) in pyridine, 0.2 M TBAP.

Figure S3). Only the spectral changes in DMSO are for the "real" compounds, those in pyridine being those of liberated [LM] where M = Zn^{II} or Cu^{II}.

The isosbestic points in the spectra in DMSO indicate the lack of detectable intermediates upon going from the neutral form of the complexes $[(PdCl_2)_4LZn]$ (Figure 6) and $[(PdCl_2)_4LCu]$ (Supporting Information, Figure S3) to the corresponding −1 charged species. There is also a common evolution of the spectra expressed by the disappearance of the Q band and the appearance of new bands at about 475−480, 550−580, and 700−740 nm in addition to a broad absorption in the region 800−900 nm. These features are common to those of the corresponding species [LZn] and [LCu] in pyridine (Figure 6 and Supporting Information, Figure S3), and also in general for other [LM] species,[2a,5a] in keeping with the assumption of ligand-centered reductions.

Conclusions

The present study describes the synthesis and physicochemical characterization of the heteropentametallic porphyrazine compounds $[(PdCl_2)_4LM]$ where M = Zn^{II}, Cu^{II}, $Mg^{II}(H_2O)$, or Cd^{II} and L = tetrakis-2,3-[5,6-di(2-pyridyl)pyrazino]porphyrazinato dianion. The properties of [LCd] and $[L'Cd]^{8+}$ (L′ = octamethylated L) are also detailed for the first time. Structural information obtained from analysis of the NMR spectra suggests that samples of the pentanuclear complexes $[(PdCl_2)_4LM]$ prepared in DMSO are composed of a largely prevalent isomer carrying the exocyclic dipyridino-$PdCl_2$ fragments which are out-of plane and oriented on the same side of the pyrazinoporphyrazine macrocyclic framework (4:0 isomer, C_{4v} symmetry). There is also a minor isomer present, likely to be a 2:2 component (cis or trans). UV−visible spectral and electrochemical data provide unequivocal evidence that external palladation influences the HOMO−LUMO energy gap and makes the macrocycles more easily reduced. This is a direct effect of the enhanced electron withdrawing properties of the peripheral fragments consequent to palladation, in line with similar effects seen for the [LM] species when changed to their corresponding octacations $[L'M]^{8+}$.

Acknowledgment. The support of the Robert A. Welch Foundation (K.M.K., Grant E-680) and the University of "La Sapienza" MIUR (C.E., Cofin 2003038084) and the Ministero dell'Università e della Ricerca Scientifica (MIUR, PRIN 2007XWBRR4) is gratefully acknowledged. E.V. was partly financed by the Consorzio Interuniversitario di Ricerca in Chimica dei Metalli nei Sistemi Biologici (CIRCMSB) for a grant during her doctoral work. Thanks are expressed to Prof. F. Monacelli for useful discussions and to Dr. Graziella Pinto for assistance in the writing of the paper.

Supporting Information Available: Figures S1 (structure of the Pd^{II} complex $[(CN)_2Py_2PyzPdCl_2]$), Figure S2 (CV in DMSO and pyridine of $[(PdCl_2)_4LCu]$ and [LCu]), Figure S3 (UV−visible spectral changes during the first one-electron reduction of $[(PdCl_2)_4LCu]$ in DMSO and [LCu] in pyridine), and Scheme S1 (possible structural isomers for the macrocycles). This material is available free of charge via the Internet at http://pubs.acs.org.